DE-FC21-94MC31388--13

DOE/MC/31388--13-Pt.4

Task 9 - Centrifugal Membrane Filtration

Semi-Annual Report
April 1 - September 30, 1997

By
Daniel J. Stepan
Michael E. Grafsgaard

Work Performed Under Contract No.: DE-FC21-94MC31388

For

U.S. Department of Energy
Office of Environmental Management
Office of Technology Development
1000 Independence Avenue
Washington, DC 20585

U.S. Department of Energy
Office of Fossil Energy
Federal Energy Technology Center
P.O. Box 880
Morgantown, West Virginia 26507-0880

By
University of North Dakota
Energy & Environmental Research Center
P. O. Box 9018
Grand Forks, North Dakota 58202-9018

Disclaimer

DISCLAIMER

Portions of this document may be illegible electronic image products. Images are produced from the best available original document.

TABLE OF CONTENTS

LIST OF FIGURES i

1.0 BACKGROUND 1

2.0 OBJECTIVES 1

3.0 ACCOMPLISHMENTS 2
- 3.1 Alternative Turbulence Promoter Design Development 2
  - 3.1.1 Hydrodynamics of Filter Cake Buildup 2
  - 3.1.2 Crossflow Filtration Evaluation 7
  - 3.1.3 Practical High-Shear Disk Membrane System Configurations 8
  - 3.1.4 Fluid Flow in Rotating Disk Systems 8
  - 3.1.5 Turbulence Promoter Design 10
- 3.2 Alternate Promoter Fabrication 14
- 3.3 Preliminary Testing 15

4.0 FUTURE WORK 16

5.0 REFERENCES 16

LIST OF FIGURES

1 Dead-end and crossflow filtration methods 3

2 Predicted flow pattern within the pressure housing 11

3 Original turbulence promoter 13

4 Angled blade turbulence promoter 14

TASK 9 – CENTRIFUGAL MEMBRANE FILTRATION

1.0 BACKGROUND

This project is designed to establish the utility of a novel centrifugal membrane filtration technology for the remediation of liquid mixed waste streams at U.S. Department of Energy (DOE) facilities in support of the DOE Environmental Management (EM) program. The Energy & Environmental Research Center (EERC) has teamed with SpinTek Membrane Systems, Inc., a small business and owner of the novel centrifugal membrane filtration technology, to establish the applicability of the technology to DOE site remediation and the commercial viability of the technology for liquid mixed waste stream remediation.

The technology is a uniquely configured process that makes use of ultrafiltration and centrifugal force to separate suspended and dissolved solids from liquid waste streams, producing a filtered water stream and a low-volume contaminated concentrate stream. This technology has the potential for effective and efficient waste volume minimization, the treatment of liquid tank wastes, the remediation of contaminated groundwater plumes, and the treatment of secondary liquid waste streams from other remediation processes, as well as the liquid waste stream generated during decontamination and decommissioning activities.

2.0 OBJECTIVES

The overall project consists of several integrated research phases related to the applicability, continued development, demonstration, and commercialization of the SpinTek centrifugal membrane filtration process. This phase of work is a continuation of the Phase 1 evaluation of the SpinTek centrifugal membrane filtration technology. During Phase 1 testing conducted at the EERC using the SpinTek ST-IIL unit operating on a surrogate tank waste, a solids cake developed on the membrane surface. Solids cake development was observed where linear membrane velocities were less than 17.5 feet per second and resulted in a reduction of unobstructed membrane surface area of up to 25%, reducing overall filtration performance.

The primary goal of the Phase 2 research effort is to enhance filtration performance through the development and testing of alternative designs of the turbulence promoters to generate a shear force across the entire membrane surface that is sufficient to maintain a self-cleaning membrane capability and improve filtration efficiency and long-term performance. Specific Phase 2 research activities include the following:

- System modifications to accommodate an 11-inch-diameter, two-disk rotating membrane assembly
- Development and fabrication of alternative designs to the existing turbulence promoters
- Testing and evaluation of the existing and alternative turbulence promoters under selected operating conditions using a statistically designed test matrix

- Data reduction and analysis

3.0 ACCOMPLISHMENTS

3.1 Alternative Turbulence Promoter Design Development

Development of alternative turbulence promoters included investigation of the hydrodynamics of filter cake buildup, examination of crossflow filtration methods, including high-shear crossflow filtration, and an evaluation of fluid flow in rotating disk systems.

3.1.1 Hydrodynamics of Filter Cake Buildup

Classical filtration, also called dead-end filtration, has traditionally been the most widely used filtration process. This method removes suspended particulate by drawing the fluid through a filter medium that retains the suspended material. As the process continues, a cake of filtered material forms on the original filter, growing at a rate proportional to the rate of fluid filtration and concentration of the slurry. The filter may soon become clogged with filtered particulate, drastically reducing the filtration rate. The initial rate of filtration can be attained by stopping the process and removing the cake. This type of filtration works well for small filtration requirements and will always be the method of choice when recovery of the suspended material is what is sought from filtration, but it becomes impractical when continuous filtration is required.

A filtration method that continuously removes the filter cake is used when continuous filtration is required. This method, called crossflow or tangential flow filtration, involves moving a fluid tangentially to a filter while simultaneously filtering it. The tangential flow creates a force parallel to the filter that helps to wash filtered particles away, thereby keeping the filter clean and the permeate flux high. Opposing the parallel shear force generated by the crossflow is the drag force caused by permeate passing over the filtered particles and through the membrane. The higher the flux, the faster the flow perpendicular to the membrane and the stronger the drag force. Particles become deposited on the filter when the drag force acting upon them becomes higher than the shear force pulling them away.

Figure 1, taken from Cardew and Byrne (1), gives an excellent visualization of dead-end and crossflow filtration methods.

Particles deposited on the filter soon form a gel or filter cake layer that can be several magnitudes lower in permeability than the original filter, restricting the flow through it (2). This restriction results in a decrease in permeate flux and its associated drag force. Eventually, an equilibrium occurs between the crossflow and the drag forces. The thickness and permeability of the gel layer when this equilibrium occurs determines the steady-state flux of the filter.

The inevitability of filter cake development during crossflow filtration has prompted numerous studies in this area. Once formed, the properties of the cake rather than that of the

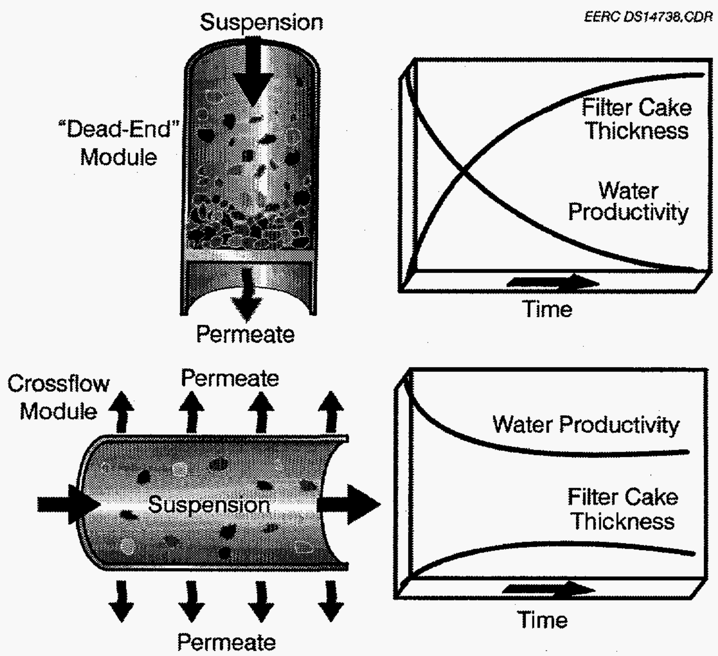

Figure 1. Dead-end and crossflow filtration methods (Source: Cardew and Byrne).

original filter may control the filtration process. Since the cake permeability can be several magnitudes lower than that of the original filter, its development can significantly decrease filtrate flux. The cake can also play a crucial role in particle rejection due to its decreased pore size over the original filter.

Forces involved in cake formation during crossflow filtration are identified by Jiao and Sharma (2) as a hydrodynamic tangential force (shear stress) created from the crossflow, a drag force resulting from the filtrate flux, a hydrodynamic lift force, and surface forces between the particle and the filter. Surface forces, although large in some instances, act over a much shorter range than the other forces. They can also be reduced by utilization of membranes that are enhanced to treat a particular waste stream (3, 4). Lift forces have been shown to be small for laminar flow over particles attached to a smooth wall (2).

Various equations for identifying the hydrodynamic forces exerted on spherical particles during crossflow filtration have been proposed. Lu and Ju (5) identify hydrodynamic forces acting upon particles during crossflow filtration as

1. Vertical drag force pulling the particulate toward the filter

$$F_{(n+w)} = \phi 3\pi\mu d_p(q - \upsilon_1) + \pi/6(\rho_p - \rho_s)gd_p^3$$

and

2. Tangential crossflow force pushing particles parallel to the filter

$$F_t = 1.7009[3\pi\mu d_p u_p(z = d_p/2)]$$

where:

ϕ = correction factor of Stokes law
μ = viscosity of fluid ($kg/s \cdot m$)
d_p = diameter of particle (m)
q = permeate flux ($m^3/s \cdot m^2$)
υ_l = lift velocity of sphere near bounded wall (m/s)
ρ_p, ρ_s = density of particle and slurry, respectively (kg/m^3)
u_p = undisturbed flow velocity at $z = d_p/2$

Utilizing the above formulas and summing the moments created by each about a contact point between the particle and the filter surface, one obtains

$$M = (d_p / 2) [F_t \cos \theta - (F_n + F_w) \sin \theta]$$

where:

M = moment created by hydrodynamic forces
θ = the angle of repose between filter and particle (rad)

The particle may remain stable on the filter (negative moment) or be swept away (positive moment). At the equilibrium point where the net moment is zero, the above equation can be solved for the largest diameter of particle that is likely to be deposited upon the filter under the given flow conditions. By making some generalized assumptions, the authors give equations for the largest critical cutoff particle diameter for turbulent and laminar flow conditions. This diameter corresponds to the largest particle that can theoretically be deposited on the membrane under the given flow conditions. Particles smaller than the cutoff diameter can become deposited on the filter, while larger particles are swept away with the crossflow.

Jiao and Sharma (2) also offer equations for the normal drag force driving the particle to the filter (F_y) and the tangential force acting to remove the particle from the filter surface (F_x). They evaluated two different mechanisms by which particles could be released from the filter: sliding and rolling. If the particle were released from the membrane by sliding, the tangential force would have to be greater than the product of the hydrodynamic drag force and the coefficient of friction between the particle and the filter. If the particle were released by rolling, which is the case for spherical particles on a flat surface (2), a torque balance should be used to evaluate whether or not the particle becomes deposited on the membrane.

Numerous investigators (2, 5, 6) have shown that the cutoff diameter is a function of filtrate flux and crossflow velocity, with higher flux corresponding to deposition of larger particles. Development of the filter cake initially begins with the deposition of a wide variety of particle sizes on the membrane, with finer and finer particles subsequently deposited. The finer particles decrease the permeability of the filter until the flux decreases to such an extent that all of the particles present within the suspension are too large to be deposited on the filter. At this point, a steady filtration rate (or steady state) is reached (2). A possible explanation for this phenomenon is as follows:

As filtration begins on a clean membrane, filtration rates are high as a result of the high permeability of the bare membrane. The large flux values correspond to increased drag forces on the particles in the slurry. The large drag forces in turn correspond to an increased critical cutoff diameter for particles to be deposited. A wide variety of particle sizes can thus be initially trapped on the filter surface. As filtration continues, more and more particles become trapped on the filter, eventually restricting flow through it. The decreased flux results in less particle drag and a smaller cutoff diameter for particles deposited on the filter. This process continues until the filtration rate is low enough that all of the remaining particles in the slurry are larger than the cutoff diameter, at which time steady state is reached (2). Further investigations have shown that filtration pressure has no effect on the steady-state filtration rate since cake permeability decreases as filtration pressure increases (2). Therefore, the filter cake acts as a secondary membrane capable of controlling the filtration process. In many cases, this layer may act as the primary filter, removing particulate from the fluid stream before it comes in contact with the original filter. Such is the case when filter aids are used. The aids develop a cake layer on the underlying filter that provides a barrier to trap unwanted particulate from going through the filter with the filtrate. These membranes are also referred to as dynamic membranes, since they develop and change continuously with the motion of the fluid being filtered.

Tanny categorized secondary membranes into three classes. These classes are summarized by Murkes and Carlsson (7) in the following manner:

Class 1 Dynamic Membranes

This class of dynamic membranes consists of those formed when a solution containing a macromolecular gel-forming solute is ultrafiltered through a membrane whose pore size is small enough to retain at least a portion of the molecule. Retention of the molecules increases their concentration from that in the bulk fluid (C_b) to an increased concentration at the membrane (C_w). As filtration continues, this concentration increases until a gel is formed, at concentration C_g, which is a constant. Mathematically, the filtrate flux (J) in this system can be expressed as

$$J = k \ln (C_w/C_b)$$

where k is a back-diffusion mass-transfer coefficient. As the concentration increases at the membrane surface, C_w approaches C_g. The flux then becomes a function of $\ln C_b$ only. Another expression for flux, written in terms of transmembrane pressure (ΔP), hydraulic resistance of the membrane (R_m), and polarization layer (R_p) is

$$J = \Delta P / (R_m + R_p)$$

By combining these flux equations, it can be shown that as long as C_w is less than that of C_g, C_w will increase with pressure. However, as soon as C_w becomes equal to C_g, increasing pressure corresponds only to an increased resistance of the gel layer and not an increase in flux.

Class 2 Dynamic Membranes

Development of this type of secondary membrane is often the case during crossflow filtration and is most probably the one formed in the SpinTek unit. This class of secondary membranes is formed from filtration of colloidal suspensions through a membrane whose pore size may be up to 1–2 μm larger than that of the colloid. Rejection of solute particles occurs through a dense layer of retained particles that form on top of the membrane. Development of the initial cake is not well understood. However, it seems that the filtered particulate first fills the membrane pores and then forms a filter cake, which subsequently rejects particles much smaller than the original filter pore size.

Mathematical models describing the filtration process where Class 2 membranes are developed include the standard law of filtration and Ruth's law. It would seem that the standard law of filtration would be valid during the initial stages of filtration, when particles smaller than the membrane pore openings become deposited within the pores at such a rate that the volume of the pores decreases in proportion to the volume filtered. This law can be expressed mathematically as

$$kt = (t / V) - (1 / J_o)$$

where J_o is the initial flux, t is the filtration time, and V is the total filtrate quantity collected until time t.

After a certain amount of filtration, clogging of the pores causes the membrane to reject almost all colloids in the suspension, and the process becomes a cake filtration process that can be represented by Ruth's law:

$$J(t) = K / (2(V+V_f))$$

In this expression, V_f represents the volume of filtrate that produces a cake having the same hydrodynamic resistance as that of the clean filter. J(t) represents the flux at time t, and K is the Ruth constant:

$$K = 2PS^2/\mu cr$$

where S is the surface area of the cake, μ is the viscosity of the fluid, c represents the concentration of the colloid, and r is the specific cake resistance (flow resistance per unit mass of solids per unit area) (7).

Class 3 Dynamic Membranes

This class of secondary membrane is formed when the solution contains molecules of a size relatively close to that of the porous support membrane. Filtration causes the molecules to enter the membrane pore, and interaction between the molecule and the membrane holds it there. The pore size of the original membrane must be very small if the held molecule is a polymer and the rejection properties of the membrane are very high. Development of this type of membrane is dependent upon the pore size of the original filter. If the pore size is too small, no particles will be trapped, while pores that are too large do not allow retention of the polymer molecules.

In almost all filtration processes, the development of a secondary or dynamic membrane is inevitable. Utilizing methods to control it may be one of the best method to enhance filtration performance. The dynamic layer can provide a barrier between the tangential shear force and the filter, protecting the filter from wear. The secondary membrane can also improve filtration by acting as a prefilter before the fluid passes through the membrane. Filtration methods should be developed to take advantage of any benefits that a gel layer may have in any crossflow application.

3.1.2 Crossflow Filtration Evaluation

The means of developing the shear force required to remove particulate from the membrane surface can be divided into two categories: low-shear crossflow filtration and high-shear crossflow filtration (7). Low-shear methods use flow velocity as the mechanism for solids cake reduction. The shear force required to keep the particles suspended in the crossflow is a function of the feed stream pumping rate. Large feed streams are required because flow velocity downstream of the feed inlet can be reduced by the removal of permeate as the feed passes across the membrane. The available shear is lowest near the downstream edge of the membrane, while the solids concentration is highest at that point because of the removal of permeate. Therefore, low-shear methods employ large pumping rates and high recirculation ratios.

The shear force in low-shear crossflow filters can be increased by utilizing unsteadiness in the crossflow. Crossflow instabilities can result from 1) roughness, where protuberances are placed on or near the filter surface, 2) flow pulsations in the feed stream, and 3) secondary flows where filter geometry is chosen to help generate Taylor and Dean vortices (8). Experiments by Mackley and Sherman (8) have shown these methods to increase flux and efficiency in low-shear systems.

Although the low-shear technique works well in many applications of waste treatment, it is ineffective for wastes containing a high percentage of solids. The high solids content overwhelms the membrane, clogging the flow passages and rendering the membrane useless. In such cases high-shear filtration methods should be used. These types of systems utilize a different technique to create shear and are designed to operate under high solids loadings with lower pumping rates than low-shear techniques. Instead of relying on high feed stream velocities to promote shear, mechanical methods are used, including moving the filter relative to the fluid (as with SpinTek) or imparting velocity to the feed water in close proximity to the filter by spinning disks or other mechanical devices. Whichever shear-promoting means is chosen, the result tends to be a much more effective filter cleaning. Since the energy is applied in the direct vicinity of the membrane, little is wasted on fluid farther away from it.

3.1.3 Practical High-Shear Disk Membrane System Configurations

High-shear filtration devices exist in two basic geometries: a rotating disk in a housing and a rotating cylinder in a housing (7). Of these, the rotating disk is the best known and most widely used because of its simplicity and the ability to pack large amounts of membrane area into a compact unit. The following are typical configurations used in high-shear filtration devices:

- Rotating disk membranes consecutively layered adjacent to stationary membranes (RMSM). This system operates on the principle that the rotating disks give an angular velocity to the fluid, which imparts a shear to keep the stationary filter disks clean. The shear imparted to the stationary filter in turn slows the fluid, causing a return shear on the rotating disks. This system packs large amounts of membrane area into a small unit. However, experiments by Wronski et al. (9) show the filtration rates of the stationary disks to be small in comparison to that of the spinning filter disks.

- Rotating disk membranes with opposing stationary shear devices (RMSS). This type of system packs less membrane area per chamber volume, but offers the advantage of increased shear along the rotating membrane. Whereas stationary filter disks are smooth and offer little resistance to fluid rotating within the spinning filter, the stationary shear–enhancing devices can be of varying geometry to promote shear and enhance flow characteristics within the filter chamber. An advantage of a system such as this is that energy is applied directly to the filter rather than to fluid away from the membrane.

- Stationary disk membranes with opposing rotating shear-promoting devices (SMRS). These units utilize rotating disks placed in close proximity to stationary membranes to develop the necessary shear to help reduce membrane fouling. Although the energy is not supplied directly to the membrane in a system such as this, the filtrate does not have to overcome the centrifugal forces developed within spinning membranes.

- Oscillating disk Membranes (OM). In these units, the membrane's rotation is changed so frequently that the process fluid is not allowed to attain the speed of the membrane. Since the fluid's speed never attains that of the membrane, high-velocity gradients occur near the membrane surface. The high-velocity gradient generates considerable shear along the membrane, giving this system high fouling resistance characteristics.

3.1.4 Fluid Flow in Rotating Disk Systems

To identify possible solutions to the filter cake development in the central portion of the rotating membrane within the SpinTek unit, an investigation of flow patterns within a housing containing a spinning disk was carried out. Substantial research has been conducted in this area (7, 10–13), although none was found that identically matched SpinTek's case. Most research has centered on spinning disks within a housing containing a fluid without permeation, although some has been conducted with the bottom of the housing made of porous medium, and tests with permeation have been run.

To describe flow patterns within a housing containing a rotating disk with radius R, and angular velocity ω, two Reynolds numbers are used (7). The first Reynolds number is dependent upon the gap width, s, between the disk and housing and the kinematic viscosity of the fluid ν.

$$Re_s = \omega s^2 / \nu$$

The second Reynolds number is dependent upon the radial distance, r, from the spinning axis.

$$Re_r = \omega r^2 / \nu$$

Spinning the disk within the housing can generate the following four different modes of fluid flow (7,12).

Region I: Laminar Flow and Narrow Gap

$Re_s \leq 4, \qquad Re_r \leq 2 \times 10^5$

In this flow regime, the laminar boundary layers are merged and produce a shear rate that varies inversely with the disk–housing gap, s.

Region II: Laminar Flow and Wide Gap

$Re_s \geq 4, \qquad Re_r \leq 2 \times 10^5$

The boundary layers within this region are separated by a zone of fluid that moves as a solid unit with rotational speed of $K\omega$, where $0 < K < 1$. The shear developed within this region is independent of the gap separating the disk and housing.

Region III: Turbulent Flow and Narrow Gap

$Re_r \geq 2 \times 10^5 \qquad s/r \leq 0.05$

The flow within this region is characterized by merged turbulent boundary layers.

Region IV: Turbulent Flow and Wide Gap

$Re_r \geq 2 \times 10^5 \qquad s/r \geq 0.05$

Two separate turbulent boundary layers are separated by a turbulent core of fluid moving at an angular velocity of $K\omega$, where $0 < K < 1$.

The K value in these descriptions is the ratio of the tangential velocity of the core to that of the spinning disk. Experiments show this value to be 0.4–0.5 for a smooth disk and up to 0.9 for a disk having eight radial vanes (7).

Correlating to the above regions, Schiele, in Murkes and Carlsson, gives the shear stresses in each region:

$$\tau_1 = \mu\, \omega\, r / s$$
$$\tau_2 = 1.81\, \rho\, \nu^{1/2}\, (K\omega)^{3/2}\, r$$
$$\tau_3 = 0.008\, \rho\, (\omega\, r)^{7/4}\, (\nu/s)^{1/4}$$
$$\tau_4 = 0.057\, \rho\, \nu^{1/5}\, (K\omega)^{9/5}\, r^{8/5}$$

where μ and ρ are the fluid dynamic viscosity and density, respectively (7).

In practice, high-shear dynamic filters operate with Reynolds numbers between 10^5 and 10^6. Adequate clearance between the spinning disk and stationary housing or filter is maintained to prevent equipment damage, so the likely flow regime in high-shear filters is Region IV (7, 12, 14). Whereas shear stress in Region IV is independent of the gap width s, if the equipment did operate in Region III, the decrease in the disk–filter gap would increase the local shear stresses according to the above formulas.

Experiments by Shirato et al. (10) show the fluid movement within a fluid housing containing a spinning disk. Along the disk, the flow is tangential through the friction developed between the disk and fluid, and radial due to centrifugal forces throwing the fluid toward the periphery of the disk. To compensate for the outward flow along the spinning disk, fluid flow near the housing is rotated inward toward the center of the chamber.

Assuming the spinning membrane to be the spinning disk and the turbulence promoters to represent the housing, it should be reasonable to assume outward flow along the membrane and inward flow along the turbulence promoters, as shown in Figure 2. It is important to note that the flow patterns within the housing are complicated by the variety of flows within it, including permeate entering the spinning membrane, feed inflow and concentrate outflow, and circulating flow within the membrane packs.

3.1.5 Turbulence Promoter Design

The analysis of flow patterns within the filter chamber was used to develop alternative turbulence promoter designs. The complex nature of flow within the chamber made a complete detailed analysis impractical. However, a basis for describing typical flows with the filtration chamber was found using research done on flow boundaries next to rotating disks. Experiments have shown the velocity of a fluid within a filter chamber containing a smooth, grooveless disk (in this case, the spinning filter) to comprise three regions: a boundary layer of thickness δ next to the spinning disk, a boundary layer of thickness ζ next to a fixed plate, and a core region between the two boundary layers. Suggestions for equations identifying flow velocity estimation within each of the layers for both laminar ($Re < 3 \times 10^5$) and turbulent flow ($Re > 3 \times 10^5$) where $Re = r_o^2\omega/\nu$ have been proposed (10).

Flows normally encountered with high-shear dynamic filtration tend to be turbulent (7, 12), because of the high energy transfer from disk to fluid. An approximation for the flow patterns of

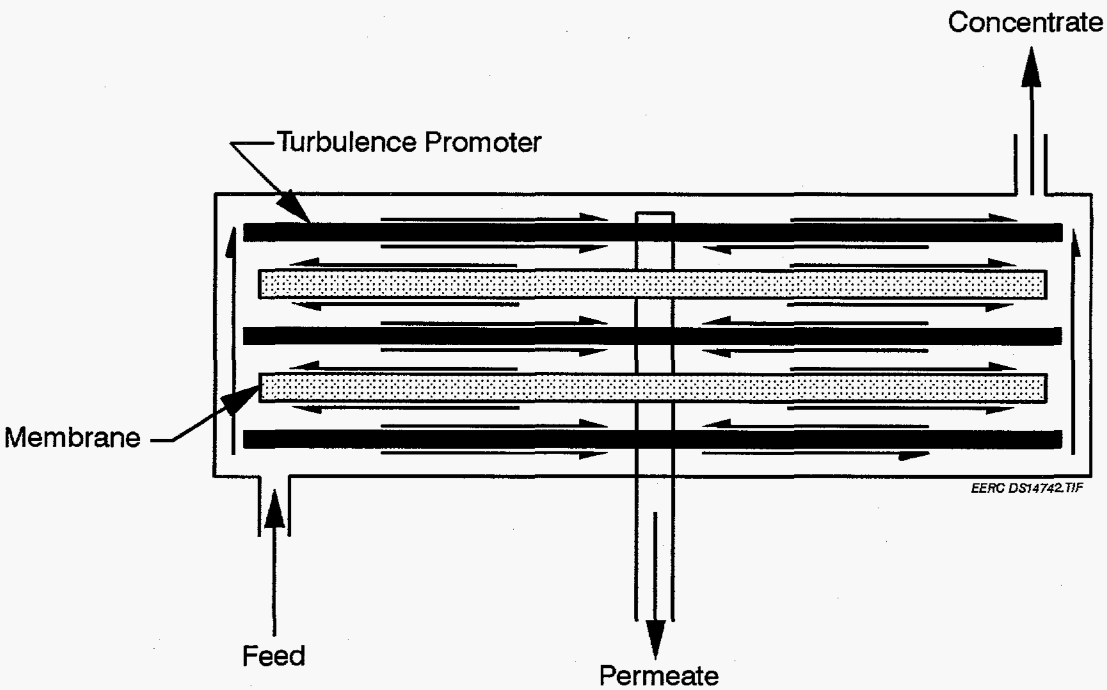

Figure 2. Predicted flow pattern within the pressure housing.

a smooth spinning disk under turbulent flow conditions was described by the following equations (10):

Fixed plate boundary layer:

Boundary layer thickness (ζ) = $0.309[r(1 - K)^3/K](\nu/r^2\omega_o)^{1/5}$ [1]

Tangential velocity (μ) = $Kr\omega_o(s/\zeta)^{1/7}$ [2]

Radial velocity (υ) = $-0.374Kr\omega_o(s/\zeta)^{1/7}(1 - s/\zeta)$ [3]

Spinning disk boundary layer:

Boundary layer thickness (δ) = $0.526(1 - K)^2 r(\upsilon/r^2{}_o\omega_o)^{1/5}$ [4]

Tangential velocity (μ) = $r_o\omega_o[1 - (z/\delta)^{1/7}+K(z/\delta)^{1/7}]$ [5]

Radial velocity (υ) = $0.220(1 - K)r_o\omega_o(z/\delta)^{1/7}(1 - z/\delta)$ [6]

where:

K = μ/r is the ratio of tangential velocities in the core and on the spinning disk, approximately 0.4 to 0.5 for a smooth disk

ω_o = the angular velocity of the disk
ν = the kinematic viscosity of the fluid
z = the axial distance from the spinning disk
r = the radial distance from the center of the disk

Equations 1–6 were used to identify methods that could enhance the flow patterns within the filter chamber to increase both circulation and shear. Assuming the turbulence promoter to be the stationary plate, one could expect turbulent flow at much lower Reynolds numbers because of the effects of the promoter blades.

To reduce cake deposition on the membrane, the disk boundary layer thickness should be kept to a minimum, decreasing the chance for particles to be trapped within it by the permeate flux drag force. Reducing the boundary layer size while increasing the radial velocities of the fluid next to the promoter should result in a sweeping action within the chamber that extracts particles before they are deposited on the membrane.

Experiments performed on spinning grooved disks have shown that the grooving increases the tangential and radial velocities of fluids next to them (10). The velocity increases were thought to be caused by the increased friction between the disk and fluid brought about by the grooves. Radial flow along the grooves was thought to be the cause of the increased radial velocities. Assuming the tractive force can be created by bladed projections as well as grooves, the feasibility of placing blades directly on the spinning filter disk to help reduce filter cake buildup was examined. Although blades on the filter disk may slightly decrease membrane area, the area lost would be small, since only a few blades should be required. To be effective, however, stationary membrane filter disks would have to replace the current turbulence promoters. The spinning filter with blades could be used to impart the shear necessary to keep the stationary filter free of deposits while increasing fluid circulation within the entire filter chamber.

The numerous drawbacks of this type of design however, may make it impractical. A net decrease in shear along the membrane could occur due to the blades increasing the amount of fluid spinning with the disk. Power consumption would be increased, as more energy is being imparted to the fluid. Furthermore, experiments performed by Wronski et al. (9) show the filtration rate of the stationary disk in such a system to be small in comparison to that of the spinning disk. Finally, system modifications would be required for such a design.

Reducing the boundary layer thickness may also be accomplished by reducing the clearance between the membrane and promoter. Although small clearance adjustments for filtration units with rotating shear promoters and stationary filter disks have resulted in only small flux changes, no evidence of the same occurrence for rotating filter disks was found. Experiments by Schiele described in Murkes and Carlsson (7) on rotating disks showed increased local shear stresses with decreased clearance for various operating conditions. The shear stress increase should result in less particle deposition and a higher flux. The increased shear stress may increase power consumption, but may be required only within the central portion of the membrane where lower local velocities and the highest permeation drag forces are present. The practical limit of clearance reduction is unknown, but adequate clearance must be maintained to prevent membrane–promoter contact during operation.

The current turbulence promoter, pictured in Figure 3, appears to be well-suited for creating shear along the membrane. The stationary blades increase velocity gradients and turbulence along the membrane, resulting in a decreased solids cake. However, although turbulence and shear are high, the circulation of fluid in and out of the disks may be small. Assuming the primary flow patterns are outward fluid flow along the spinning membrane and feed inflow along the stationary blades, this configuration may not provide enough circulation for solutions with a high solids content. Low circulation may cause excessive solids concentrations within the filter disks, resulting in unavoidable filter cake formation.

Incorporating a promoter design that increases flow circulation within the chamber may also help decrease gel layer formation. A promoter having angled blades, such as the one pictured in Figure 4, should help increase fluid circulation within the chamber. This type of design could help to remove particles from within the filtration disks by imparting a radial velocity to fluid particles having a tangential velocity component. The radial velocity increase could help expel particles from the central portion of the membrane, while helping bring fresh waste to the disks for filtration.

Creating a bevel on the leading edge of the turbulence promoter blades may also be useful in limiting filter cake buildup. Beveling the edge, alternately on top, then bottom, for consecutive blades may allow the blade to create lift and turbulence to help increase shear and reduce the

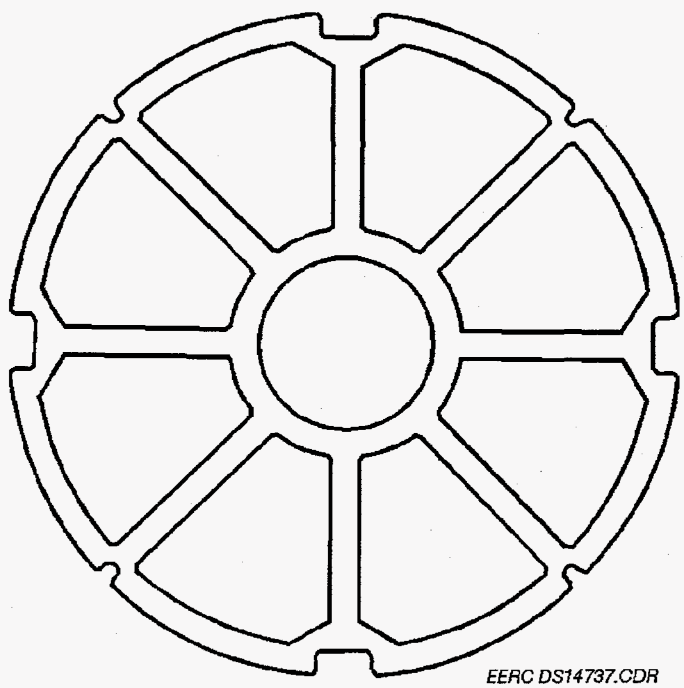

Figure 3. Original turbulence promoter.

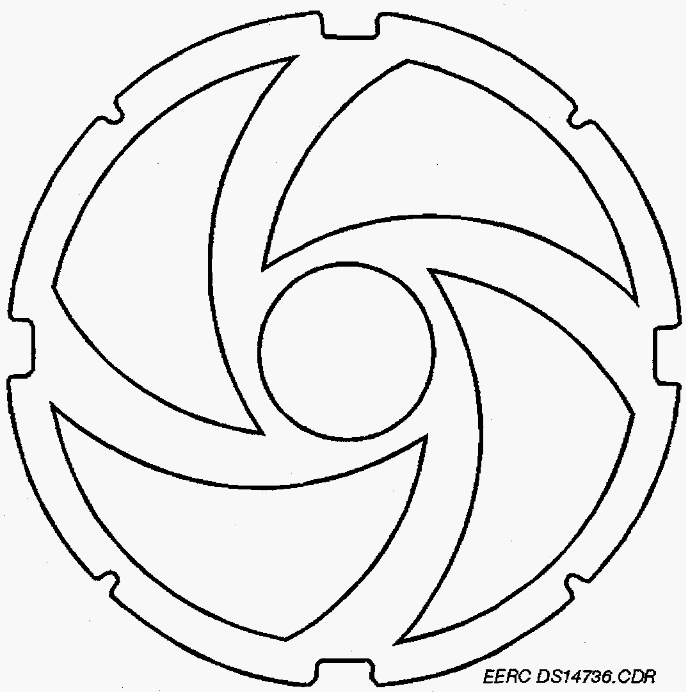

Figure 4. Angled blade turbulence promoter.

solids cake. The beveling effect may not be pronounced on the original promoter design, but using thicker promoters with a smaller membrane–promoter gap may magnify the beveling effect.

3.2 Alternate Promoter Fabrication

A new promoter design was created utilizing a CAD drawing of a current turbulence promoter. Use of the current drawing ensured a proper fit within the unit, decreasing the chance of equipment damage. Three new promoters sets were cut from stainless steel using a computer-guided plasma cutter. One set of promoters was cut utilizing the original design, but was 0.0675 in. thicker than the original. The two other sets were both of the new design, but one was equal to the original promoter thickness of 0.120 in., while the other's thickness was increased to 0.1875 in. Thickness variation allowed flux testing as a function of membrane–promoter clearance. Utilizing two thicknesses of each design allowed testing of permeate flux as a function of membrane–promoter gap as well as design efficiency.

The thicker promoters were then machined using a CNC milling machine. Removing 0.0625 in. off of each side of the promoter from the outer perimeter to a distance of 1 in. inside it increased clearance to allow for the outer adhesive bead on the membrane. All newly cut promoters were then cleaned to remove any remaining steel shavings that could possibly damage test equipment.

3.3 Preliminary Testing

The first test trials were performed using tap water. This permitted testing of the membranes to ensure membrane integrity and helped to fill pores in the new membrane to reduce permeate flux. Running the tap water on the membranes reduced the flux from 1400 gallons per square foot per day (gfd) on the fresh disks to about 650 gfd. If actual testing were started on the fresh membrane disks, a very high solids concentration could develop within the filter housing because of such a high removal of permeate, causing decreased system performance and possible equipment damage. Testing the tap water also allowed clearance testing of all promoters involved in the trials before the statistical test matrix was begun.

Initial testing was started using a 20 wt % calcium carbonate suspension and the original turbulence promoter, at the following test variables:

Feed Pressure (psi)	Feed Temperature (°F)	Feed Flow (Lph)	Rotor Speed (rpm)
60	100	600	1200

After flow was established through the unit and the membrane housing pressurized as in normal operation, the system shut down just after the rotor was started. Removing the cover on the membrane housing showed a complete solids cake within the filter chamber, overwhelming the membranes. This high solids concentration within the chamber increased the torque on the rotor to such an extent that the motor's thermal safety shutoff engaged, stopping the system.

It was thought that the high solids buildup may have been due to inadequate flow through the housing resulting from the positioning of the concentrate piping, which was directly above the feed line. The majority of flow, it was thought, was going directly out the concentrate, completely bypassing the membranes and causing an inevitable solids buildup within the chamber. Any flow reaching the membrane would be dewatered by removal of permeate, and the lack of adequate crossflow would not flush the solids out with the concentrate. To test this theory, the concentrate line was moved to the opposite side of the housing. Moving the line decreased the possibility of the test solution flowing through the chamber without coming in contact with the membranes.

Moving the line proved to decrease solids within the housing and the decreased torque on the rotor did not cause system shutdown. However, during further testing, samples taken from the concentrate line appeared to have a blue tint, signifying abrasion of the membrane. Upon checking the permeate flux, it was noted that it had almost doubled from that which occurred with tap water. The system was immediately shut down. All of this occurred within a few minutes of start-up. Removing the housing cover showed a high solids loading within the filter chamber, although not to the same extent as before the line was moved. Inspection of the membranes showed almost complete membrane deterioration. Only a small amount of the membrane surface remained at the center, while only the porous steel backing was left on the outer edge.

A subsequent test run was performed on two new membranes after they had been tested with tap water. The new trial was on the same calcium carbonate suspension, but additional water was added to decrease the solids concentration to 10 wt %. It was felt that diluting the test solution would decrease solids concentrations within the membrane housing and stop the membrane abrasion. The new test run used the same operating parameters as the first except for the decreased solids loading. During the run, the system operated without difficulty, producing clear permeate and no noticeable blue color in the concentrate. A log of the flux however, showed a steady increase from the initial 636 gfd to over 1100 gfd in less than 1 hour of operating time. After operating a total of 4 hours, the membranes were once again almost completely abraded.

After the problem was discussed with Richard Hayes Jr. from SpinTek, he ran tests of his own. His investigation showed that the abrasion was probably a membrane phenomenon rather than a system deficiency, owing to a change in their method of manufacture.

Further testing has yet to be performed because of the membrane abrasion problems. It is anticipated that testing will begin shortly, dependent upon the arrival of hardened membranes.

4.0 FUTURE WORK

Continued work on this task will involve testing and process evaluation using the original wagon wheel and the angled blade design turbulence promoters. A statistical test matrix will be utilized, with test runs being conducted in a randomized order. Temperature and solids loading will be held constant at 90°F and 25 wt%. Two different pressure conditions (40 and 60 psig) and two rotor speeds (900 and 1200 rpm) will be the process variables. Performance will be measured by flux (gal/ft^2-day) and power consumption (kWh). Total run time will also be monitored to account for any irreversible membrane fouling. The test matrix requires 25 individual test runs, each of which will be conducted over a 4-hour test period with a minimum of 2 hours of steady-state data collection. Based on the results of statistical analyses of test data, further design modifications to the turbulence promoters will be evaluated, followed by additional testing and analysis.

5.0 REFERENCES

1. Cardew, P.; Byrne, M. "Scale-up of Crossflow Filters: Reducing the Risks," F*iltration and Separation*, **1995**, *June* 493–498.

2. Jiao, D.; Sharma, M.M. "Mechanism of Cake Buildup in Crossflow Filtration of Colloidal Suspensions," *Journal of Colloid and Interface Science* **1994**, *162,* 454–462.

3. Rolchigo, P. M. "Filtration Basics," *Industrial Wastewater*, **1997**, *January/February* 35–40.

4. Holeschovsky, U.; Cooney, C. "Quantitative Description of Ultrafiltration in a Rotating Filtration Device," *ALCHE Journal* **1991**, *37* (8), 1219–1226.

5. Lu, Wei-Ming; Ju, Shang-Chung. "Selective Particle Deposition in Crossflow Filtration," *Separation Science and Technology* **1989**, *24* (7, 8), 517–540.

6. Su-Jiang, Yazhen; Dodds, J.; Leclerc, D. "Cake Characteristics in Crossflow and Dead-End Microfiltration," *Filtration and Separation* **1995**, *September*, 795–798.

7. Murkes, J.; Carlsson, C.G. *Crossflow Filtration*; John Wiley & Sons Ltd., 1988.

8. Mackley, M.R.; Sherman, N.E. "Cross-Flow Filtration with and Without Cake Formation," *Chemical Engineering Science* **1994**, *49*, 171–178.

9. Wronski, S.; Molga, E.; Rudniak, L. "Dynamic Filtration in Biotechnology," *Bioprocess Engineering* **1989**, *4*, 99–104.

10. Shirato, M.; Murase, T.; Yamazaki, H.; Iwata, M.; Inayoshi, M. "Patterns of Flow in a Filter Chamber During Dynamic Filtration with a Grooved Disk," *International Chem. Eng.* **1987**, *27*, 304–310.

11. Watabe, Komei. "Experiments on the Fluid Friction of a Rotating Disc with Blades," *Bulletin of JSME* **1962**, *5* (17), 49–57.

12. Lee, S.S.; Burt, A.; Russotti, G.; Buckland, B. "Microfiltration of Recombinant Yeast Cells Using Rotating Disk Dynamic Filtration System," *Biotechnology and Bioengineering* **1995**, *48*, 386–400.

13. Lu, Wei-Ming; Chuang, Ching-Jung. "Effect of Permeation Through Stator on the Hydrodynamics of a Rotating Disk Dynamic Filter," *Journal of Chemical Engineering of Japan* **1988**, *21* (4), 368–374.

14. Wronski, S.; Mroz, A. "Power Consumption in Dynamic Disc Filters," *Filtration and Separation* **1984**, *November/December* 397–399.